Materials Views
www.MaterialsViews.com

ADVANCED MATERIALS
www.advmat.de

Influence of Alkyl Chain Branching Positions on the Hole Mobilities of Polymer Thin-Film Transistors

*Ting Lei, Jin-Hu Dou, and Jian Pei**

Conjugated polymers have great potential for use in flexible, large-area and low-cost optoelectronic devices due to their solution processability and superior mechanical properties.[1] Nevertheless, charge mobilities in polymeric field-effect transistors (PFETs) are generally low due to poor packing and lack of macroscopic order.[2,3] To solve this problem, an effective solution is the rational design of new polymers based on deep insight into the structure–property relationship, which is unfortunately rare in comparison to small molecules used in organic field-effect transistors (OFETs).[4] Most efforts have been focused on the design of building blocks for polymer backbones,[1–3] and little research has shed light on the influence of molecular weight,[5] building block symmetry,[6] and alkyl side chains[7,8] on charge mobilities.

Alkyl chains have been demonstrated to play important roles in intermolecular interactions and supramolecular self-assembly.[9] Generally, alkyl side chains are attached onto conjugated polymers as solubilizing groups to ensure polymer solubility in organic solvents. Recently, more and more attention has been devoted to engineering alkyl chains in conjugated polymers. The chain type and length as well as substituting position on conjugated polymers have crucial consequences on molecular packing and thin-film morphology, and hence on device performance.[10] Compared to linear alkyl chains, branched alkyl chains, such as 2-ethylhexyl, 2-hexyldecyl, 2-octyldodecyl, and 2-decyltetradecyl groups, can provide better solubility for polymers.[2,3] Surprisingly, the distance of the branching point of all these branched alkyl chains to the conjugated backbone is not longer than one methylene group, presumably because these branched alkyl chains are readily available. To increase the structural diversity of solubilizing groups, Bao et al. designed an unconventional siloxane-terminated hexyl chain. The polymer formed with this group exhibited closer backbone packing and increased hole mobility in comparison to that with the conventional 2-octyldodecyl group.[7a] Although the concept of moving the branching point away from the polymer backbone has been demonstrated, the trimethylsilyl group cannot survive under certain conditions,[11] hence limiting the application of this elegantly designed group. Moreover, the structural difference to conventional branched alkyl chains is drastic.

An electron-deficient isoindigo unit has been developed by Reynolds and Anderson et al. for polymer solar cells.[12] We recently used isoindigo-based conjugated polymers as the active layers for air-stable PFETs,[13] and found that modification of the main chain by a "molecular docking" strategy and tuning of polymer symmetry led to systematically high mobility.[6a] This type of polymer was also used by Bao et al. and the mobility was improved further.[7a] Herein, we add a 2-octyldodecyl group and three novel-designed branched alkyl chains (3-decyltridecyl, 4-decyltetradecyl, and 5-decylpentadecyl) to our isoindigo-based conjugated polymer (**Scheme 1**). We investigate how moving the branching point further from the backbone influences the mobilities. The sequential changing of these "more conventional" branched alkyl chains results in a remarkably high mobility of 3.62 cm^2 V^{-1} s^{-1}. Thus, we demonstrate that a subtle change to the conventional alkyl chains can lead to significant improvement of device performance.

Scheme 1 illustrates the synthetic route to these polymers. Synthesis of the monomers is shown in detail in the Supporting Information. Interestingly, the R_f values of **IID-C3** and **IID-C4** from thin layer chromatography (TLC) (0.52 for **IID-C3** and 0.53 for **IID-C4**) are significantly smaller than those of **IID** and **IID-C2** (0.61 for both, Figure S1, Supporting Information). It is likely that the polar carbonyl groups in the isoindigo core are somewhat shielded by the alkyl side chains, and moving the branched point away exposes these polar groups, thus leading to stronger interaction of the monomer with the silica gel. Similar to the preparation of polymer **IIDDT**,[13] the Stille-coupling polymerization between dibromide **IID-C2**, **IID-C3**, or **IID-C4** and 5,5′-bis(trimethylstannyl)-2,2′-bithiophene was employed to afford **IIDDT-C2**, **IIDDT-C3**, and **IIDDT-C4** in high yields. All polymers were obtained as dark metallic solids after careful purification of precipitation into methanol and subsequent Soxhlet extraction with acetone, hexane, and chloroform. Molecular weights of all polymers were evaluated by gel permeation chromatography (GPC) with 1,2,4-tricholorobenzene (TCB) as the eluent at 150 °C (**Table 1**). **IIDDT-C3** and **IIDDT-C4** appear to have larger molecular weight (M_n) and polydispersity index (PDI) because of shoulder peaks in the large molecular weight region (Figure S2, Supporting Information). These shoulder peaks are presumably due to interpolymer aggregations. All polymers show good thermal stability with decomposition temperatures over 370 °C. No phase transition was observed for all polymers by differential scanning calorimetry (DSC) in the range of –10 to 300 °C (Figure S3, Supporting Information).

Absorption spectra of all polymers and monomers were measured both in solution and in thin film. All monomers

---

T. Lei, J.-H. Dou, Prof. J. Pei
Beijing National Laboratory for Molecular Sciences
The Key Laboratory of Bioorganic Chemistry and
Molecular Engineering of Ministry of Education
College of Chemistry and Molecular Engineering
Peking University
Beijing 100871, China
E-mail: jianpei@pku.edu.cn

DOI: 10.1002/adma.201202689

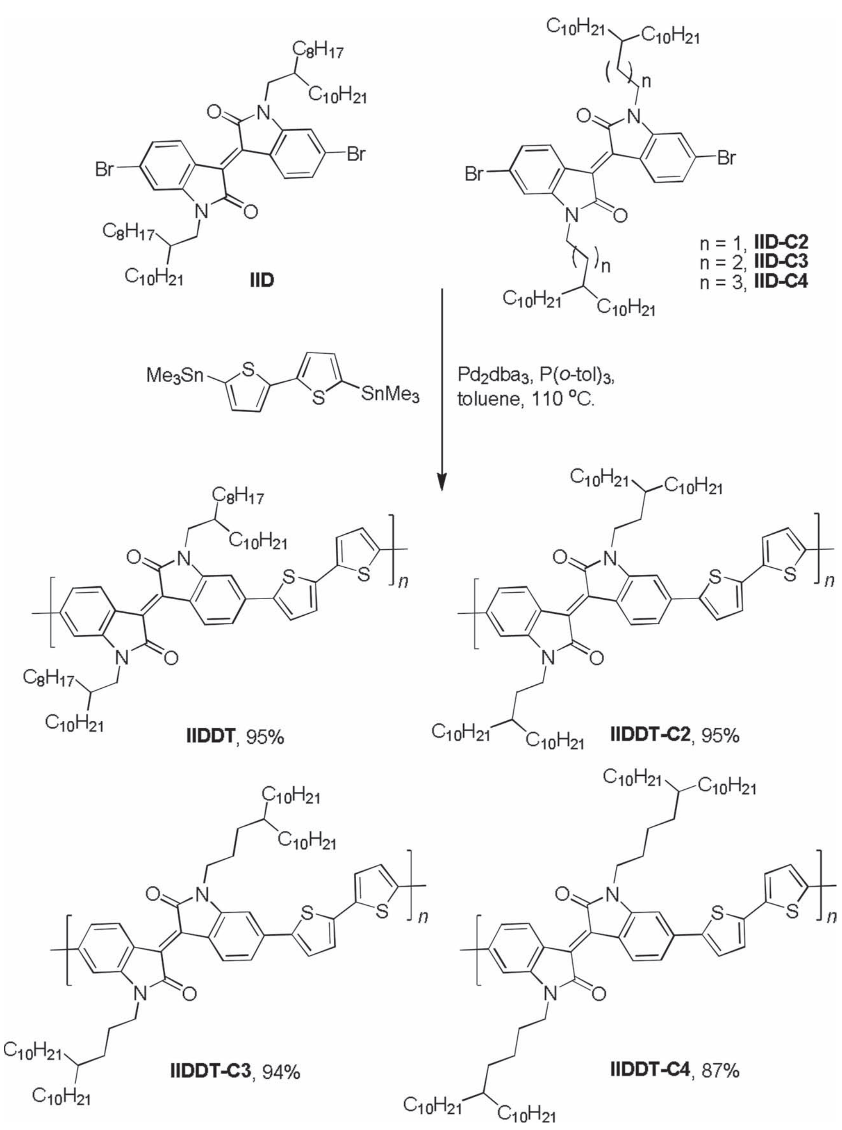

Scheme 1. Synthesis of polymers **IIDDT** and **IIDDT-C(2–4)**, with varying branched position of alkyl side chains.

show almost identical absorption spectra (Figure S4, Supporting Information), suggesting that the alkyl chains do not affect the photophysical properties of the aromatic core. All polymers show typically dual band absorption (**Figure 1**). Compared with **IIDDT** and **IIDDT-C2**, **IIDDT-C3** and **IIDDT-C4** show marked red-shifted absorption in solution. The red-shift may be attributed to interpolymer π–π stacking, which makes the polymer backbone of **IIDDT-C3** and **IIDDT-C4** more planar. This result is consistent with the GPC result that **IIDDT-C3** and **IIDDT-C4** exhibit some aggregation even at 150 °C. Absorption peaks of all polymers in thin film show an interesting blue-shift (especially *0–1* vibrational peaks) in comparison with those in solution, which may correlate with their solid state packing. Scrutiny of spectra reveals that the *0–0* vibrational transition increases, whereas *0–1* decreases in the film, suggesting that polymers become more planar in the film with enhanced π–π stacking. Annealing the films leads to a further slightly increase of the *0–0* vibrational absorption, indicating that the packing and planarity of the polymers are improved (Figure S5 in the Supporting Information and Table 1).

The cyclic voltammograms (CV) were used to evaluate electronic energy levels of the polymers. All polymers show much stronger oxidative peaks than their reductive ones, almost one order of magnitude higher, indicating that these polymers are more easily oxidized than reduced (**Figure 2**). Moving the branching point away from the polymer backbones leads to a noticeable increase of the HOMO levels from –5.70 eV (**IIDDT**) to –5.50 eV (**IIDDT-C4**). However, the LUMO levels show only a slight decrease from –3.70 eV (**IIDDT**) to –3.74 eV (**IIDDT-C4**). This result may be again due to the more planar backbone and better stacking in **IIDDT-C3** and **IIDDT-C4**. The computational study also reveals that the LUMOs of the polymers are localized on isoindigo core, whereas HOMOs are distributed along the polymer chain (Figure S6, Supporting Information). Thus, HOMO levels of the polymers are more easily affected by their conformational change. Photoelectron spectroscopy (PES) was also used to measure the HOMO energy levels of all polymers. Similar variation trends were found, thus further confirming

Table 1. Optical and Electrochemical Properties of Polymers.

Polymers	M_n [kDa]/PDI	T_d [°C]	λ_{max}^{sol} [nm]^{a}	λ_{max}^{film} [nm]	E_g^{opt} [eV]^{b}	E_{HOMO} [eV]^{c}	E_{LUMO} [eV]^{c}	E_g^{CV} [eV]^{d}	E_{HOMO}^{PES} [eV]
IIDDT	20.4/2.0	390	706, 647	701, 637	1.60	–5.70	–3.70	2.00	–5.54
IIDDT-C2	18.4/2.0	384	711, 647	707, 641	1.60	–5.60	–3.70	1.90	–5.57
IIDDT-C3	39.2/3.2	392	718, 673	719, 653	1.58	–5.52	–3.74	1.78	–5.33
IIDDT-C4	37.3/2.3	374	719, 675	716, 647	1.58	–5.50	–3.74	1.76	–5.26

[a] 10^{-5} M in chloroform; [b] Estimated from the onset of thin-film absorption; [c] Cyclic voltammetry determined with Fc/Fc$^+$ (E_{HOMO} = –4.80 eV) as the external reference; [d] $E_g^{CV} = E_{LUMO} – E_{HOMO}$.

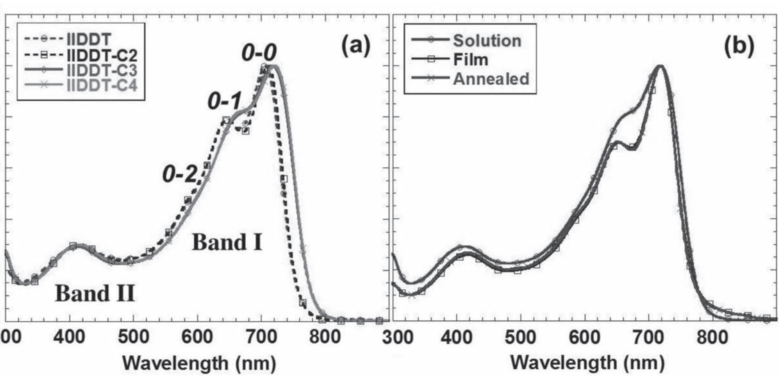

Figure 1. Normalized UV-vis absorption spectra of a) polymers in $CHCl_3$ (1×10^{-5}M) and b) **IIDDT-C3** in $CHCl_3$ (1×10^{-5}M), in thin film, and in annealed film (at 150 °C for 30 min).

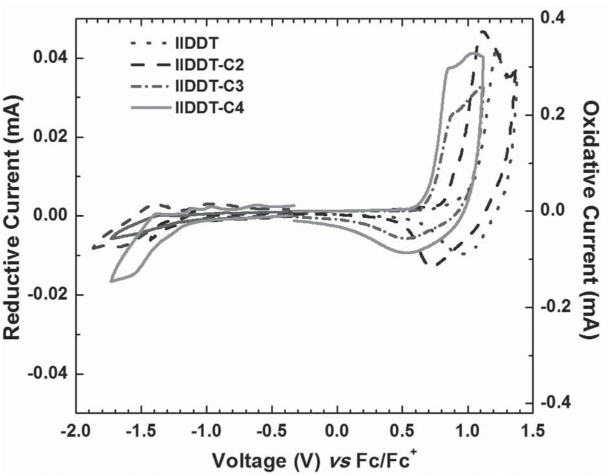

Figure 2. Cyclic voltammograms of polymers in thin film drop-casted on a glassy carbon electrode and tested in n-Bu_4NPF_6/CH_3CN solution (scan rate: 50 mV s^{-1}).

the CV results (Figure S7 in the Supporting Information and Table 1).

It is known that charge carrier mobility in OFETs strongly depends on the frontier orbital overlap integrals. The overlap integrals are sensitive to π–π stacking distance and molecular packing conformation.[14] To probe how moving the alkyl chain branching point influences the charge transport of the polymers, we fabricated bottom-gate/top-contact field-effect devices. A thin layer of polymers was deposited on octadecyltrimethoxysilane (OTS)-treated SiO_2 (300 nm)/n^{++}-Si substrate by spin-coating a polymer solution (4 mg/mL in 1,1,2,2-tetrachloroethane) at 1000 rpm for 40 s. In our previous report, **IIDDT** films showed an average hole mobility of 0.66 cm^2 V^{-1} s^{-1} and a maximum mobility of 1.06 cm^2 V^{-1} s^{-1}.[6a] In contrast, **IIDDT-C3** films exhibited a mobility up to 3.62 cm^2 V^{-1} s^{-1} and an average mobility of 2.98 cm^2 V^{-1} s^{-1} after annealing at 175 °C for 30 min (**Figure 3**). This result is among the highest hole mobilities of polymers reported to date.[5a,7a,8] **IIDDT-C4** films also displayed increased mobility: the highest mobility was up to 1.76 cm^2 V^{-1} s^{-1} and the average mobility was 1.44 cm^2 V^{-1} s^{-1} (Figure S8, Supporting Information). Unexpectedly, **IIDDT-C2** films showed decreased device performance compared with **IIDDT** films. The highest mobility of **IIDDT-C2** films was only 0.40 cm^2 V^{-1} s^{-1} (**Table 2**). Recently, Müllen et al. reported that molecular weight played an important role in improving hole mobilities.[5a] We were aware of the relatively low M_n of **IIDDT** and **IIDDT-C2**, hence we synthesized the polymer **IIDDT-C3** with a M_n of 20 kDa, comparable to those of **IIDDT** and **IIDDT-C2**. Films of **IIDDT-C3** also showed the highest hole mobility (>3 cm^2 V^{-1} s^{-1}), thus further confirming the significant effect of moving the branching point away. Nonetheless, increased M_n of **IIDDT-C3** and **IIDDT-C4** may still contribute to their high hole mobilities. In addition, similar to other isoindigo-based polymers,[6a,7a,13] **IIDDT-C3** and **IIDDT-C4** also displayed good stability under ambient conditions (R_H = 50–60%) for at least two months (Figure S9, Supporting Information).

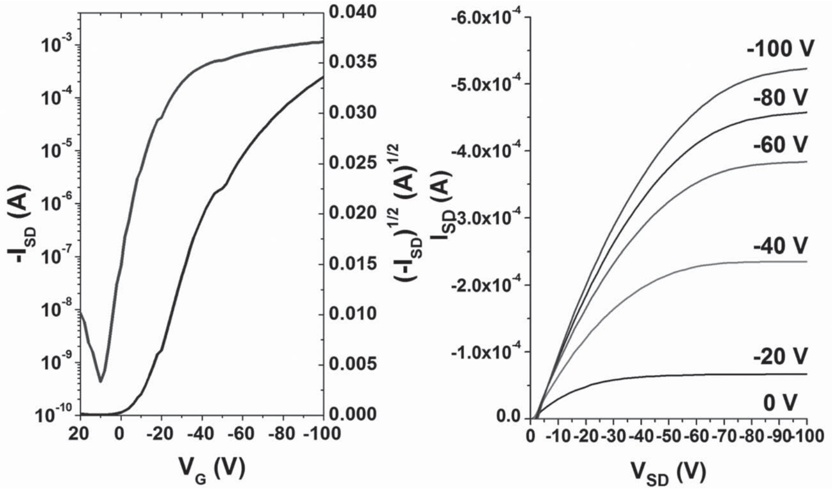

Figure 3. Transfer (left) and output (right) characteristics of **IIDDT-C3** devices (spin-casted from TCE solutions, 4 mg/mL) at V_{SD} = –100 V (L = 60 μm, W = 3.0 mm) after thermal annealing. The hole mobility in the saturation regime was calculated from the slopes obtained by linear fitting of $(I_{SD})^{1/2}$ vs V_G in the V_G range from –21 to –30 V.

The high hole mobilities of **IIDDT-C3** and **IIDDT-C4** are likely due to a more exposed isoindigo core and stronger π–π interactions of polymer backbones. To gain further understanding, we employed grazing incidence X-ray diffraction (GIXD) and tapping-mode atomic force microscopy (AFM) to investigate polymer packings and film morphologies. As shown in **Figure 4**, **IIDDT-C3** displays a strong out-of-plane diffraction at 2θ of 2.88°, corresponding to a d-spacing of 24.7 Å (λ = 1.2398 Å). The other four diffractions are attributed to the (200),

Table 2. OFET Device Performances and GIXD Results of Polymers.

Polymers	$T_{\text{annealing}}$ [°C]	μ [cm^2 V^{-1} s^{-1}]^{a}	V_t [V]	$I_{\text{on}}/I_{\text{off}}$	d [Å]$^{b)}$	
					L	π
IIDDT	150	1.06 (0.66)	–18	$>10^6$	20.3	3.75
IIDDT-C2	200	0.40 (0.28)	–10	$>10^5$	23.7	3.61
IIDDT-C3	175	3.62 (2.98)	–2	$>10^6$	24.7	3.57
IIDDT-C4	175	1.76 (1.44)	–5	$>10^6$	26.1	3.57

[a)] Measured under ambient condition ($R_H \approx$ 50–60%). Maximum values of hole mobilities, and average mobilities are shown in parentheses (more than 10 devices were tested); [b)] Lamellar (L) and π–π stacking (π) distances determined by GIXD experiments.

(300), (400), and (500) diffractions, indicating that **IIDDT-C3** has a long-range ordered edge-on lamellar packing. **IIDDT-C2** and **IIDDT-C4** also show similar out-of-plane lamellar packing with *d*-spacing of 23.7 and 26.1 Å, respectively. Their *d*-spacings correlate well with their alkyl chain lengths, suggesting the alkyl side chains all adopt a similar extended conformation in films. Compared with **IIDDT-C3**, **IIDDT** shows markedly broader diffractions and only four lamellar diffraction peaks. Thus, polymer packings in **IIDDT-C3** film are more ordered. In the in-plane diffractions, the π-stacking diffractions of polymers (010) are observed. After moving the branching point away from backbone, the polymers show gradually decreased π–π stacking distances (3.75 Å for **IIDDT**, 3.61 Å for **IIDDT-C2**, and 3.57 Å for both **IIDDT-C3** and **IIDDT-C4**). **IIDDT-C3** also displays more intense (010) diffractions, suggesting stronger π-stacking interactions. In addition, diffraction halos of alkyl chains are also observed in the range of 4–5 Å, much larger than π-stacking distances. Therefore, largely improved mobilities are likely due to decreased π-stacking distances. AFM images of the polymer films show crystalline fibrillar intercalating networks (Figure S11, Supporting Information). The crystalline networks are likely the result of strong intermolecular π–π interactions, similar to other high performance OFET materials.[3]

In Bao's work, the polymer with a hole mobility of 2.48 cm^2 V^{-1} s^{-1} had a π–π stacking distance of 3.58 Å, and the reference polymer had a mobility of 0.57 cm^2 V^{-1} s^{-1} and a distance of 3.76 Å.[7a] In Liu's work, the DPP-based polymer with 2-decyltetradecyl group gave a record-breaking high mobility of 8.2 cm^2 V^{-1} s^{-1} with a π–π stacking distance of 3.66 Å, and the reference polymer with the 2-octyldodecyl group had a mobility of 4.5 cm^2 V^{-1} s^{-1} and a distance of 3.72 Å.[8] Our results further substantiate these results, as **IIDDT-C3** shows the highest mobility (3.62 cm^2 V^{-1} s^{-1}) and the shortest distance (3.57 Å). On the other hand, although π-stacking distances of **IIDDT**–**IIDDT-C4** decrease with the moving branching positions, their mobilities do not always increase correspondingly. For instance, π-stacking distance of **IIDDT-C2** (3.61 Å) is considerably shorter than that of **IIDDT** (3.75 Å), but the mobility of **IIDDT-C2** (0.40 cm^2 V^{-1} s^{-1}) is lower than that of **IIDDT** (1.06 cm^2 V^{-1} s^{-1}). **IIDDT-C3** and **IIDDT-C4** both have the shortest distance (3.57 Å), but their mobilities differ (3.62 cm^2 V^{-1} s^{-1} for high M_n**IIDDT-C3**, 3.00 cm^2 V^{-1} s^{-1} for low M_n**IIDDT-C3**, and 1.76 cm^2 V^{-1} s^{-1} for **IIDDT-C4**). In addition, we are aware that in Liu's work, it is the length of alkyl chains rather than the branching position that plays a dramatic role. Thus, we prepared **IIDDT** with a 2-decyltetradecyl group and found a mobility of 0.96 cm^2 V^{-1} s^{-1} and a π–π stacking distance of 3.75 Å, almost identical to those of **IIDDT** (1.06 cm^2 V^{-1} s^{-1} and 3.75 Å). Recently, Beljonne and coworkers demonstrated that charge transport correlates with the supramolecular organization of polymers; in addition, the π-stacking distance and the packing conformation greatly affect the interpolymer chain carrier transport.[15] We propose that the stacking conformations of our polymers, such as degrees of translation and rotation, also play a critical role in carrier mobility, which resulted in the inconsistency between device performances and π-stacking distances.

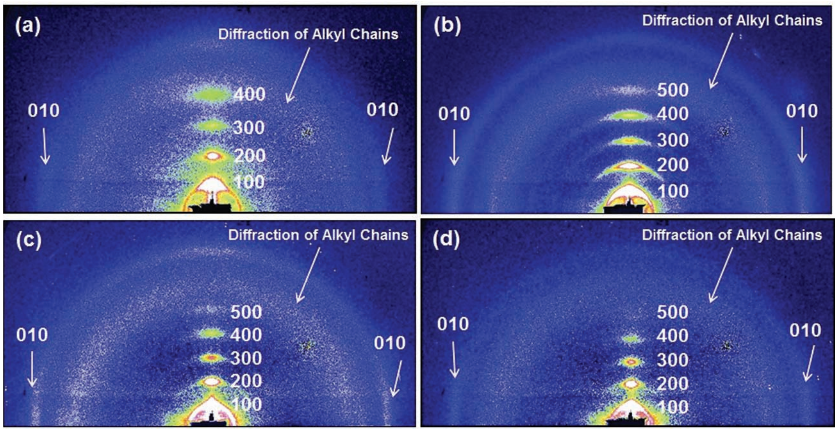

Figure 4. 2D-GIXD patterns of a) **IIDDT**, b) **IIDDT-C2**, c) **IIDDT-C3**, and d) **IIDDT-C4** film after thermal annealing (at 150 °C for 30 min). All polymers display lamellar packings.

In conclusion, we have investigated thoroughly how the branching position of alkyl side chains affects FET performance of isoindigo-based conjugated polymers. An exceptionally high mobility of 3.62 cm^2 V^{-1} s^{-1} is achieved for **IIDDT-C3**, in comparison to 1.06 cm^2 V^{-1} s^{-1} for **IIDDT** and 0.40 cm^2 V^{-1} s^{-1} for **IIDDT-C2**. The branching point variation strategy developed in this work reveals the significance of sophisticated side chain molecular engineering of conventional alkyl chains and its dependence of the backbone structures. A systematic investigation of the side chain effect, its synergy with the backbone, and other factors, such as molecular weight, is currently underway in our group.

Experimental Section

*Synthesis of **IIDDT-C2***: **IID-C2** (250 mg, 0.235 mmol), 5,5′-bis(trimethylstannyl)-2,2′-bithiophene (115.6 mg, 0.235 mmol), $Pd_2(dba)_3$ (4.3 mg, 2 mol%), P(*o*-tol)$_3$ (5.7 mg, 8 mol%), and 10 mL of toluene were added to a Schlenk tube. The tube was charged with nitrogen through a freeze-pump-thaw cycle three times. The mixture was stirred for 24 h at 110 °C. *N,N′*-Diethylphenylazothioformamide (20 mg) was then added and then the mixture was stirred for 1 h to remove any residual catalyst before being precipitated into methanol (200 mL). The precipitate was filtered through a nylon filter and purified via Soxhlet extraction for 8 h with acetone, 12 h with hexane, and finally was collected with chloroform. The chloroform solution was then concentrated by evaporation and precipitated into methanol (200 mL) and filtered off to afford a dark solid (236 mg, yield 94%). Anal. calcd: for $(C_{70}H_{104}N_2O_2S_2)_n$: C 78.52, H 9.88, N 2.62; found: C 77.78, H 9.47, N 2.55.

*Synthesis of **IIDDT-C3***: The synthetic procedure is similar as described for **IIDDT-C2** (yield 94%). Anal. calcd. for $(C_{72}H_{108}N_2O_2S_2)_n$: C 77.78, H 9.92, N 2.55; found: C 77.85, H 9.75, N 2.48.

*Synthesis of **IIDDT-C4***: The synthetic procedure is similar as described for **IIDDT-C2** (yield 87%). Anal. calcd. for $(C_{74}H_{112}N_2O_2S_2)_n$: C 78.95, H 10.03, N 2.49; found: C 78.25, H 9.91, N 2.46.

Figure S1-S12, synthesis and characterization of monomers, and polymer FET device fabrications are detailed in the Supporting Information.

Supporting Information

Supporting Information is available from the Wiley Online Library or from author.

Acknowledgements

This work was supported by the Major State Basic Research Development Program (No 2009CB623601) from the Ministry of Science and Technology, and National Natural Science Foundation of China. The authors thank beamline BL14B1 (Shanghai Synchrotron Radiation Facility) for providing the beam time.

Received: July 3, 2012
Revised: August 8, 2012

---

[1] a) F. Garnier, R. Hajlaoui, A. Yassar, P. Srivastava, *Science* **1994**, *265*, 1864; b) H. Sirringhaus, N. Tessler, R. H. Friend, *Science* **1998**, *208*, 1741; c) H. Sirringhaus, T. Kawase, R. H. Friend, T. Shimoda, M. Inbasekaran, W. Wu, E. P. Woo, *Science* **2000**, *290*, 2123; d) H. Yan, Z. Chen, Y. Zheng, C. Newman, J. R. Quinn, F. Doltz, M. Kestler, A. Facchetti, *Nature* **2009**, *457*, 679.

[2] a) Y. Li, *Acc. Chem. Res.* **2012**, *45*, 723; b) C. Wang, H. Dong, W. Hu, Y. Liu, D. Zhu, *Chem. Rev.* **2012**, *112*, 2208; c) P. M. Beaujuge, J. M. J. Fréchet, *J. Am. Chem. Soc.* **2011**, *133*, 20009; d) Y. Wen, Y. Liu, *Adv. Mater.* **2010**, *22*, 1331; e) J. Chen, Y. Cao, *Acc. Chem. Res.* **2009**, *42*, 1709.

[3] a) H. Usta, C. Newman, Z. Chen, A. Facchetti, *Adv. Mater.* **2012**, *24*, 3678; b) I. Osaka, M. Shimawaki, H. Mori, I. Doi, E. Miyazaki, T. Koganezawa, K. Takimiya, *J. Am. Chem. Soc.* **2012**, *134*, 3498; c) I. Osaka, M. Akita, T. Koganezawa, K. Takimiya, *Chem. Mater.* **2012**, *24*, 1235; d) J. D. Yuen, J. Fan, J. Seifter, B. Lim, R. Hufschmid, A. J. Heeger, F. Wudl, *J. Am. Chem. Soc.* **2011**, *133*, 20799; e) H. Bronstein, Z. Chen, R. S. Ashraf, W. Zhang, J. Du, J. R. Durrant, P. S. Tuladhar, K. Song, S. E. Watkins, Y. Geerts, M. M. Wienk, R. A. J. Janssen, T. Anthopoulos, H. Sirringhaus, M. Heeney, I. McCulloch, *J. Am. Chem. Soc.* **2011**, *133*, 3272; f) Y. Li, P. Sonar, S. P. Singh, M. S. Soh, M. van Meurs, J. Tan, *J. Am. Chem. Soc.* **2011**, *133*, 2198; g) Y. Li, S. P. Singh, P. Sonar, *Adv. Mater.* **2010**, *22*, 4862; h) X. Zhan, Z. Tan, B. Domercq, Z. An, X. Zhang, S. Barlow, Y. Li, D. Zhu, B. Kippelen, S. R. Marder, *J. Am. Chem. Soc.* **2007**, *129*, 7246.

[4] a) A. N. Sokolov, S. Atahan-Evrenk, R. Mondal, H. B. Akkerman, R. S. Sánchez-Carrera, S. Granados-Focil, J. Schrier, S. C. B. Mannsfeld, A. P. Zoombelt, Z. Bao, A. Aspuru-Guzik, *Nat. Commun.* **2011**, *2*, 437; b) K. Takimiya, S. Shinamura, I. Osaka, E. Miyazaki, *Adv. Mater.* **2011**, *23*, 4347; c) J. E. Anthony, *Angew. Chem. Int. Ed.* **2008**, *47*, 452; d) J. E. Anthony, *Chem. Rev.* **2006**, *106*, 5028.

[5] a) H. N. Tsao, D. M. Cho, I. Park, M. R. Hansen, A. Mavrinskiy, D. Y. Yoon, R. Graf, W. Pisula, H. W. Spiess, K. Müllen, *J. Am. Chem. Soc.* **2011**, *133*, 2605; b) R. J. Kline, M. D. McGehee, E. N. Kadnikova, J. Liu, J. M. J. Fréchet, *Adv. Mater.* **2003**, *15*, 1519; c) A. Zen, J. Pflaum, S. Hirschmann, W. Zhuang, F. Jaiser, U. Asawapirom, J. P. Rabe, U. Scherf, D. Neher, *Adv. Funct. Mater.* **2004**, *14*, 757; d) R. Zhang, B. Li, M. C. Iovu, M. Jeffries-EL, G. Sauvé, J. Cooper, S. Jia, S. Tristram-Nagle, D. M. Smilgies, D. N. Lambeth, R. D. McCullough, T. Kowalewski, *J. Am. Chem. Soc.* **2006**, *128*, 3480; e) I. McCulloch, M. Heeney, M. L. Chabiny, D. DeLongchamp, R. J. Kline, M. Cölle, W. Duffy, D. Fischer, D. Gundlach, B. Hamadani, R. Hamilton, L. Richter, A. Salleo, M. Shkunov, D. Sparrowe, S. Tierney, W. Zhang, *Adv. Mater.* **2009**, *21*, 1091.

[6] a) T. Lei, Y. Cao, X. Zhou, Y. Peng, J. Bian, J. Pei, *Chem. Mater.* **2012**, *24*, 1762; b) M. He, J. Li, A. Tandia, M. Sorensen, F. Zhang, H. Fong, V. A. Pozdin, D.-M. Smilgies, G. G. Malliaras, *Chem. Mater.* **2010**, *22*, 2770.

[7] a) J. Mei, D. H. Kim, A. L. Ayzner, M. F. Toney, Z. Bao, *J. Am. Chem. Soc.* **2011**, *133*, 20130; b) I. Osaka, R. Zhang, G. Sauvé, D.-M. Smilgies, T. Kowalewski, R. D. McCullough, *J. Am. Chem. Soc.* **2009**, *131*, 2521; c) A. Babel, S. A. Jenekhe, *Synth. Met.* **2005**, *148*, 169.

[8] H. Chen, Y. Guo, G. Yu, Y. Zhao, J. Zhang, D. Gao, H. Liu, Y. Liu, *Adv. Mater.* **2012**, *24*, 4618.

[9] a) S. Saito, K. Nakakura, S. Yamaguchi, *Angew. Chem., Int. Ed.* **2011**, *51*, 714; b) Y. Kikkawa, E. Koyama, S. Tsuzuki, K. Fujiwara, K. Miyake, H. Tokuhisa, M. Kanesato, *Surf. Sci.* **2007**, *601*, 2520; c) L. Ding, H.-B. Li, T. Lei, H.-Z. Ying, R.-B. Wang, Y. Zhou, Z.-M. Su, J. Pei, *Chem. Mater.* **2012**, *24*, 1944.

[10] a) C. Piliego, T. W. Holcombe, J. D. Douglas, C. H. Woo, P. M. Beaujuge, J. M. J. Fréchet, *J. Am. Chem. Soc.* **2010**, *132*, 7595; b) A. T. Yiu, P. M. Beaujuge, O. P. Lee, C. H. Woo, M. F. Toney, J. M. J. Fréchet, *J. Am. Chem. Soc.* **2012**, *134*, 2180; c) W. D. Oosterbaan, J.-C. Bolée, A. Gadisa, V. Vrindts, S. Bertho, J. D'Haen, T. J. Cleij, L. Lutsen, C. R. McNeill, L. Thomsen, J. V. Manca, D. Vanderzande, *Adv. Funct. Mater.* **2010**, *20*, 792; d) J. M. Szarko, J. Guo, Y. Liang, B. Lee, B. S. Rolczynski, J. Strzalka, T. Xu, S. Loser, T. J. Marks, L. Yu, L. X. Chen, *Adv. Mater.* **2010**, *22*, 5468; e) E. Cho, C. Risko, D. Kim, R. Gysel, N. C. Miller, D. W. Breiby, M. D. McGehee, M. F. Toney, R. J. Kline, J.-L. Bredas, *J. Am. Chem. Soc.* **2012**, *134*, 6177; f) R. J. Kline, D. M. DeLongchamp, D. A. Fischer, E. K. Lin, L. J. Richter, M. L. Chabinyc, M. F. Toney, M. Heeney, I. McCulloch, *Macromolecules* **2007**, *40*, 7960.

[11] P. J. Kocieński, *Protecting Groups,* 3rd Ed., Georg Thieme Verlag, New York **2005**.

[12] a) E. Wang, Z. Ma, Z. Zhang, K. Vandewal, P. Henriksson, O. Inganás, F. Zhang, M. R. Andersson, *J. Am. Chem. Soc.* **2011**, *133*, 14244; b) Z. Ma, E. Wang, M. E. Jarvid, P. Henriksson, O. Inganäs, F. Zhang, M. R. Andersson, *J. Mater. Chem.* **2012**, *22*, 2306; c) E. Wang, Z. Ma, Z. Zhang, P. Henriksson, O. Inganäs, F. Zhang, M. R. Andersson, *Chem. Commun.* **2011**, *47*, 4908; d) R. Stalder, J. Mei, J. R. Reynolds, *Macromolecules* **2010**, *43*, 8348.

[13] T. Lei, Y. Cao, Y. Fan, C.-J. Liu, S.-C. Yuan, J. Pei, *J. Am. Chem. Soc.* **2011**, *133*, 6099.

[14] V. Coropceanu, C. Jérôme, D. A. da Silva Filho, Y. Olivier, R. Silbey, J.-L. Brédas, *Chem. Rev.* **2007**, *107*, 926.

[15] D. Niedzialek, V. Lemaur, D. Dudenko, J. Shu, M. R. Hansen, J. W. Andreasen, W. Pisula, K. Müllen, J. Cornil, D. Beljonne, *Adv. Mater.* **2012**, DOI: 10.1002/adma.201201058.